

Neutrinoless and Two-Neutrino Double-Beta Decay with Emission of Single Free Electron

A. Babič^{1,2,3}, **D. Štefánik**⁴, **M. I. Krivoruchenko**^{3,5,6},
F. Šimkovic^{2,3,4}

¹Faculty of Nuclear Sciences and Physical Engineering,
Czech Technical University in Prague, 115 19 Prague, Czech Republic

²Institute of Experimental and Applied Physics,
Czech Technical University in Prague, 128 00 Prague, Czech Republic

³Bogoliubov Laboratory of Theoretical Physics,
Joint Institute for Nuclear Research, 141980 Dubna, Russia

⁴Faculty of Mathematics, Physics and Informatics, Comenius University in
Bratislava, 842 48 Bratislava, Slovakia

⁵Institute for Theoretical and Experimental Physics, 117218 Moscow, Russia

⁶Moscow Institute of Physics and Technology, 141700 Dolgoprudny, Russia

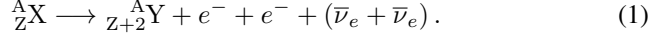
Abstract. We study a new mode of the neutrinoless and two-neutrino double-beta decays in which a single electron is emitted from the atom. The other electron is directly produced in one of the empty $s_{1/2}$ or $p_{1/2}$ orbitals of the daughter ion. The neutrinoless electron-production mode $0\nu EP\beta^-$, which would manifest through a monoenergetic peak at the endpoint of the single-electron energy spectrum, is shown to be out of reach of the currently planned experiments. Conversely, its two-neutrino counterpart $2\nu EP\beta^-$ might have already influenced the single-electron spectra measured, *e.g.*, for the isotope ^{100}Mo in the experiment NEMO-3. We discuss the prospects for detecting these new modes also for ^{82}Se in its forthcoming successor SuperNEMO.

1 Introduction

The discovery of neutrino oscillations marked the beginning of a new era in neutrino physics, main feature of which is the question of the origin and absolute scale of neutrino masses. Observation of the neutrinoless double-beta decay would imply a Majorana nature of massive neutrinos ν_i ($i = 1, 2, 3$), a consequence of which would be the identity of the flavor neutrinos ν_α ($\alpha = e, \mu, \tau$) and their respective antineutrinos $\bar{\nu}_\alpha$ [1]. Moreover, it would bring us compelling evidence that the total lepton number L is not strictly conserved in the nature. The search for this elusive process provides us with means to set upper limits on the absolute scale of neutrino masses, as well as with a unique access to the mechanism of CP violation in the lepton sector which is necessary in order to explain the observed baryon asymmetry of the Universe [2].

The observed form of the double-beta decay $2\nu\beta^-\beta^-$ involves a transmutation of an even-even parent nucleus ${}^A_Z X$ into an even-even daughter nucleus

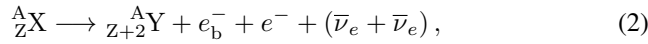
${}_{Z+2}^A\text{Y}$, accompanied by an emission of two electrons e^- and a pair of electron antineutrinos $\bar{\nu}_e$ from the atom, while in its hypothetical neutrinoless version $0\nu\beta^-\beta^-$ the antineutrinos are missing:



The neutrinoless mode $0\nu\beta^-\beta^-$ increases L by 2 units and could be discovered in calorimetric measurements of the sum of electron energies by revealing a monoenergetic peak at the two-electron spectrum endpoint corresponding to the total released kinetic energy Q . The two-neutrino mode $2\nu\beta^-\beta^-$ has so far been observed for 11 out of 35 even-even isotopes for which the ordinary β^- decay into the odd-odd intermediate nucleus is either energetically forbidden or substantially suppressed by spin selection rules [3]. In this work, we focus on the $0^+ \rightarrow 0^+$ ground-state transition of the isotope ${}^{100}\text{Mo}$ which was extensively studied throughout the operation of the tracking-and-calorimetry double-beta-decay experiment NEMO-3 located at the Modane Underground Laboratory (LSM), France [4].

In 1992, Jung *et al.* observed for a first time the bound-state β^- decay in which the electron is directly produced in atomic K or L shell and the monochromatic electron antineutrino carries away almost the entire energy of the decay [5]. The group has studied bare ${}^{163}_{66}\text{Dy}^{66+}$ ions collected in a heavy-ion storage ring at GSI, Darmstadt, and deduced a half-life of 47 d for the otherwise stable isotope. It was pointed out that such rare form of the β^- decay might play a crucial role in stellar plasma where highly-ionized atoms participate in the nucleosynthesis.

In this work, we propose to study the bound-state double-beta decay $0\nu\text{EP}\beta^-$ ($2\nu\text{EP}\beta^-$):



where a single free electron e^- is emitted from the nucleus, while the electron production (EP) of a bound electron e_{b}^- is assumed to fill one of the empty $s_{1/2}$ or $p_{1/2}$ orbitals above the valence shell of the daughter ion ${}_{Z+2}^A\text{Y}^{2+}$. Inclusion of the bound states with higher angular momenta is not necessary since their wave functions experience only a negligible overlap with the nucleus. These new single-electron modes exhibit a distinctive kinematics and could in principle be recognized by their characteristic signal induced in the double-beta-decay detectors. For instance, $0\nu\text{EP}\beta^-$ (being effectively a two-body decay) should be searched for in the form of a monoenergetic peak at the endpoint of the energy distribution of individual electrons. The single-electron spectra have been measured in the NEMO-3 experiment and will be studied with enhanced accuracy in its forthcoming successor SuperNEMO [6].

2 Calculation of Phase-Space Factors

The double-beta decay can occur in the 2nd order of the effective β -decay Hamiltonian [7]:

$$\mathcal{H}_\beta(x) = \frac{G_\beta}{\sqrt{2}} \bar{e}(x) \gamma^\mu (1 - \gamma^5) \nu_e(x) j_\mu(x) + \text{H.c.}, \quad (3)$$

where $G_\beta = G_F \cos \theta_C$ contains the Fermi constant G_F and Cabibbo angle $\theta_C = 13^\circ$ [8], $e(x)$ and $\nu_e(x)$ denote the electron and electron-antineutrino fields, respectively, and $j_\mu(x) = \bar{p}(x) \gamma_\mu (g_V - g_A \gamma^5) n(x)$ is the hadronic charged current involving the proton $p(x)$ and neutron $n(x)$ fields with the vector $g_V = 1$ and (unquenched) axial-vector $g_A = 1.269$ weak coupling constants. Due to neutrino mixing, the left-handed components of the flavor-neutrino fields $\nu_\alpha(x)$ are in fact linear combinations of the underlying massive-neutrino fields $\nu_i(x)$ given by the unitary PMNS matrix: $\nu_{\alpha L}(x) = \sum_i U_{\alpha i} \nu_{iL}(x)$.

Assuming the Majorana nature of massive neutrinos and employing the standard approximations, the formula for the inverse $0\nu\beta^-\beta^-$ half-life can be brought into the following form [1]:

$$\left(T_{1/2}^{0\nu\beta\beta}\right)^{-1} = g_A^4 G^{0\nu\beta\beta}(Z, Q) |M^{0\nu\beta\beta}|^2 \left|\frac{m_{\beta\beta}}{m_e}\right|^2. \quad (4)$$

Here, the phase-space factor $G^{0\nu\beta\beta}(Z, Q)$ depends solely on the kinematics of the involved particles, the nuclear matrix element $M^{0\nu\beta\beta}$ can be in principle determined from the theory of nuclear structure, and the effective Majorana neutrino mass $m_{\beta\beta} = \sum_i U_{ei}^2 m_i$ is a function of (yet unknown) parameters of the neutrino physics: the Majorana phases $\alpha_{1,2}$ embedded in the PMNS matrix elements U_{ei} and the neutrino masses m_i . To this day, the most stringent limits have been obtained in the ^{136}Xe double-beta-decay experiments KamLAND-Zen and EXO-200, with the former providing a constraint as low as [9]: $|m_{\beta\beta}| < 61\text{--}165\text{ meV}$. On the other hand, the formula for the inverse $2\nu\beta^-\beta^-$ half-life can be derived within the Standard Model [10]:

$$\left(T_{1/2}^{2\nu\beta\beta}\right)^{-1} = g_A^4 G^{2\nu\beta\beta}(Z, Q) |m_e M^{2\nu\beta\beta}|^2. \quad (5)$$

For the single-electron modes $0\nu\text{EP}\beta^-$ and $2\nu\text{EP}\beta^-$, their respective inverse half-lives $\left(T_{1/2}^{0\nu\text{EP}\beta}\right)^{-1}$ and $\left(T_{1/2}^{2\nu\text{EP}\beta}\right)^{-1}$ exhibit a structure fully analogous to the aforementioned, the only distinction being in the corresponding phase-space factors $G^{0\nu\text{EP}\beta}(Z, Q)$ and $G^{2\nu\text{EP}\beta}(Z, Q)$. Since these quantities depend crucially on the atomic structure, we employed a fully relativistic description of the final-state electrons in terms of the solutions to the Dirac equation with centrally-symmetric potential [11]:

$$\psi_{\kappa\mu}(\vec{r}) = \begin{pmatrix} f_\kappa(r) \Omega_{\kappa\mu}(\hat{r}) \\ i g_\kappa(r) \Omega_{-\kappa\mu}(\hat{r}) \end{pmatrix}, \quad (6)$$

where the radial wave functions $f_\kappa(r)$ and $g_\kappa(r)$ depend on the energy of the electron, while the angular functions $\Omega_{\kappa\mu}(\hat{r})$, also known as the spinor spherical harmonics, are common for both the discrete and continuous spectrum. The quantum number $\kappa = (l - j)(2j + 1) = \pm 1, \pm 2, \dots$ collectively labels all possible couplings of the orbital $l = 0, 1, \dots$ and spin $s = \pm 1/2$ angular momenta, while $\mu = -j, \dots, +j$ denotes the projection of the total angular momentum $j = |l + s|$ onto the z -axis.

For the $0\nu\text{EP}\beta^-$ and $2\nu\text{EP}\beta^-$ phase-space factors we have derived the following formulae:

$$G^{0\nu\text{EP}\beta} = \frac{G_\beta^4 m_e^2}{32\pi^4 R^2 \ln 2} \sum_{n=n_{\min}}^{\infty} B_n(Z, A) F(Z + 2, E) E p, \quad (7)$$

$$G^{2\nu\text{EP}\beta} = \frac{G_\beta^4}{8\pi^6 m_e^2 \ln 2} \sum_{n=n_{\min}}^{\infty} B_n(Z, A) \times \int_{m_e}^{m_e+Q} dE F(Z + 2, E) E p \int_0^{m_e+Q-E} d\omega_1 \omega_1^2 \omega_2^2. \quad (8)$$

In the first equation, the nuclear radius R is by convention included explicitly in order to make the nuclear matrix element $M^{0\nu\beta\beta}$ dimensionless. The factor of $\ln 2$ comes from the relation between the decay rate and half-life: $\Gamma = \ln 2/T_{1/2}$.

The quantity $B_n(Z, A)$ is a bound-state analogue of the Fermi function familiar from the theory of beta decay:

$$B_n(Z, A) = f_{n,-1}^2(R) + g_{n,+1}^2(R), \quad (9)$$

where the two terms originate from the inclusion of $s_{1/2}$ and $p_{1/2}$ bound states, respectively. In order to properly account for the relativistic many-electron structure and the shielding effect of nuclear charge, the radial wave functions $f_{n,-1}(R)$ and $g_{n,+1}(R)$ of the bound electron e_b^- at the nuclear radius $R = 1.2 \text{ fm } A^{1/3}$ were evaluated by means of the multiconfiguration Dirac–Hartree–Fock package GRASP2K [12, 13]. The computation was performed assuming the electron configuration of the parent atom ${}^A_Z X$, with the daughter isotope ${}^A_{Z+2} Y$ being the source of nuclear Coulomb attraction, for all available electron shells above the valence shell ($n_{\min} = 5$ for ${}^{100}_{42}\text{Mo}$) up to $n = 9$. Since in the absence of atomic shielding the squared electron wave functions near the origin decrease as n^{-3} [14], the rest of electron shells were to a good accuracy ($\sim 5\%$) approximated by a fit of the calculated values using the power function cn^{-p} and summed analytically via the Riemann zeta function $\zeta(p)$. Since the convergence could not be achieved in case of the $6s_{1/2}$ orbital, the value of $f_{6,-1}^2(R)$ has been replaced by the one predicted by the fit.

The Fermi function $F(Z, E)$, which involves the continuous-spectrum radial wave functions $f_{-1}(E, R)$ and $g_{+1}(E, R)$ evaluated on the nuclear surface,

can be approximated by the expression for the relativistic $s_{1/2}$ wave [15]:

$$F(Z, E) = f_{-1}^2(E, R) + g_{+1}^2(E, R) \approx 4 \left[\frac{|\Gamma(\gamma + i\nu)|}{\Gamma(2\gamma + 1)} \right]^2 (2pR)^{2\gamma-2} e^{\pi\nu}, \quad (10)$$

where $\gamma = \sqrt{1 - (\alpha Z)^2}$, $\nu = \alpha ZE/p$, and $p = |\vec{p}|$ is the momentum magnitude of the free electron e^- with energy $E = \sqrt{\vec{p}^2 + m_e^2}$. In the results, the Fermi function $F(Z + 2, E)$ assumes the full charge of the daughter nucleus ${}_{Z+2}^A Y$, since in the continuum the shielding effect has been shown to be rather insignificant [16].

In $G^{0\nu EP\beta}$, the free-electron energy is fixed by the energy conservation: $E = m_e + Q$, where we have neglected the nuclear recoil as well as the binding energy of the bound electron e_b^- . In $G^{2\nu EP\beta}$, similar approximations erase the dependence on n from the integral boundaries and, in turn, an infinite sum of integrals simplifies into a product of $\sum_{n=n_{\min}}^{\infty} B_n(Z, A)$ and just one double integral; in the integral over the first-neutrino energy ω_1 , the second-neutrino energy is once again constrained by the energy conservation: $\omega_2 = m_e + Q - E - \omega_1$.

3 Half-Lives and Single-Electron Spectra

In Table 1, we present the values of the $0\nu\beta^-\beta^-$ and $0\nu EP\beta^-$ phase-space factors $G^{0\nu\beta\beta}$ and $G^{0\nu EP\beta}$ obtained for the $0^+ \rightarrow 0^+$ ground-state transition of the isotope ${}^{100}\text{Mo}$ with total released kinetic energy $Q = 3.034 \text{ MeV}$ [17], assuming the unquenched value of the axial-vector weak coupling constant $g_A = 1.269$. We also evaluate the ratio between the corresponding decay rates: $\Gamma^{0\nu EP\beta}/\Gamma^{0\nu\beta\beta} = G^{0\nu EP\beta}/G^{0\nu\beta\beta}$, which is independent of the nuclear matrix element $M^{0\nu\beta\beta}$ and the effective Majorana neutrino mass $m_{\beta\beta}$, and hence free of the peculiarities of the nuclear and neutrino physics. Finally, we estimate the $0\nu\beta^-\beta^-$ and $0\nu EP\beta^-$ half-lives $T_{1/2}^{0\nu\beta\beta}$ and $T_{1/2}^{0\nu EP\beta}$ based on the value of the nuclear matrix element $|M^{0\nu\beta\beta}| = 5.850$ calculated in [18] via the spherical pn-QRPA approach including the realistic CD-Bonn nucleon-nucleon potential with short-range correlations and partial isospin-symmetry restoration, and assuming the value of the effective Majorana neutrino mass $|m_{\beta\beta}| = 50 \text{ meV}$ which is compatible with the inverted hierarchy of neutrino masses. The value obtained

Table 1. The $0\nu\beta^-\beta^-$ and $0\nu EP\beta^-$ phase-space factors $G^{0\nu\beta\beta}$ and $G^{0\nu EP\beta}$, decay-rate ratio $\Gamma^{0\nu EP\beta}/\Gamma^{0\nu\beta\beta} = G^{0\nu EP\beta}/G^{0\nu\beta\beta}$ and half-lives $T_{1/2}^{0\nu\beta\beta}$ and $T_{1/2}^{0\nu EP\beta}$ for the isotope ${}^{100}\text{Mo}$, assuming the nuclear matrix element $|M^{0\nu\beta\beta}| = 5.850$ [18] and the effective Majorana neutrino mass $|m_{\beta\beta}| = 50 \text{ meV}$.

$G^{0\nu\beta\beta} [\text{y}^{-1}]$	$G^{0\nu EP\beta} [\text{y}^{-1}]$	$\Gamma^{0\nu EP\beta}/\Gamma^{0\nu\beta\beta}$	$T_{1/2}^{0\nu\beta\beta} [\text{y}]$	$T_{1/2}^{0\nu EP\beta} [\text{y}]$
1.887×10^{-14}	7.400×10^{-20}	3.92×10^{-6}	6.24×10^{25}	1.59×10^{31}

for the decay-rate ratio $\Gamma^{0\nu\text{EP}\beta^-}/\Gamma^{0\nu\beta\beta^-}$ suggests a suppression of the single-electron mode $0\nu\text{EP}\beta^-$ by 6 orders of magnitude, which is mainly attributed to the presence of other electrons in the inner atomic shells: the lowest-lying orbitals (which would otherwise provide the largest contributions to the decay rate $\Gamma^{0\nu\text{EP}\beta^-}$) are already occupied, while the shielding effect of nuclear charge substantially reduces the bound-state wave functions on the surface of the nucleus. The estimated half-life $T_{1/2}^{0\nu\text{EP}\beta^-}$ further confirms that the mode $0\nu\text{EP}\beta^-$ can hardly be observed in the current and near-future experiments.

In Table 2, we show analogous results for the $2\nu\beta^-\beta^-$ and $2\nu\text{EP}\beta^-$ phase-space factors $G^{2\nu\beta\beta^-}$ and $G^{2\nu\text{EP}\beta^-}$, as well as the decay-rate ratio $\Gamma^{2\nu\text{EP}\beta^-}/\Gamma^{2\nu\beta\beta^-} = G^{2\nu\text{EP}\beta^-}/G^{2\nu\beta\beta^-}$. The $2\nu\beta^-\beta^-$ half-life $T_{1/2}^{2\nu\beta\beta^-}$ for the $0^+ \rightarrow 0^+$ ground-state transition of ^{100}Mo has been measured experimentally [3], from which the value of $g_A^2 |M^{2\nu\beta\beta^-}|$ can be deduced regardless of the details of the nuclear-structure theory, and used to predict the $2\nu\text{EP}\beta^-$ half-life $T_{1/2}^{2\nu\text{EP}\beta^-}$ without any further assumptions; for the unquenched value $g_A = 1.269$ it follows: $|m_e M^{2\nu\beta\beta^-}| = 0.1194$. We observe that the decay-rate ratio $\Gamma^{2\nu\text{EP}\beta^-}/\Gamma^{2\nu\beta\beta^-}$ indicates a relative suppression of the mode $2\nu\text{EP}\beta^-$ to be one order of magnitude lower as compared to the neutrinoless case. Moreover, the absolute half-life $T_{1/2}^{2\nu\text{EP}\beta^-}$ even turns out to fall within the sensitivity of some of the running experiments, which points to somewhat more optimistic prospects for finding the signatures of such rare decay in the available double-beta-decay detectors.

In Figure 1, we compare the calculated $0\nu\beta^-\beta^-$ and $0\nu\text{EP}\beta^-$ single-electron spectra. These are represented by differential decay rates $1/\Gamma^{0\nu\beta\beta^-} d\Gamma/dE$ (with the former normalized to unity) as functions of the electron kinetic energy $E - m_e$. In particular, we consider the $0^+ \rightarrow 0^+$ ground-state transition of the isotope ^{100}Mo with $Q = 3.034$ MeV [17], which had been extensively used in the NEMO-3 experiment [4]. From the obtained phase-space factor $G^{0\nu\text{EP}\beta^-}$ it follows that the single-electron mode $0\nu\text{EP}\beta^-$ constitutes a sharp peak at the endpoint of the $0\nu\beta^-\beta^-$ single-electron spectrum, *i.e.*, the free electron effectively carries away the entire released kinetic energy Q . For illustration purposes, we present the $0\nu\text{EP}\beta^-$ peak as a Gaussian with $\sigma = 50$ keV (which coincides with the desired energy resolution of SuperNEMO calorimeters [6]) and scale its height by a factor of 10^4 . From such disproportion it is clear that the $0\nu\text{EP}\beta^-$ peak will hardly be observed in the forthcoming measurements.

Table 2. The $2\nu\beta^-\beta^-$ and $2\nu\text{EP}\beta^-$ phase-space factors $G^{2\nu\beta\beta^-}$ and $G^{2\nu\text{EP}\beta^-}$, decay-rate ratio $\Gamma^{2\nu\text{EP}\beta^-}/\Gamma^{2\nu\beta\beta^-} = G^{2\nu\text{EP}\beta^-}/G^{2\nu\beta\beta^-}$ and half-lives $T_{1/2}^{2\nu\beta\beta^-}$ [3] (which implies the nuclear matrix element: $|m_e M^{2\nu\beta\beta^-}| = 0.1194$) and $T_{1/2}^{2\nu\text{EP}\beta^-}$ for the isotope ^{100}Mo .

$G^{2\nu\beta\beta^-}$ [y^{-1}]	$G^{2\nu\text{EP}\beta^-}$ [y^{-1}]	$\Gamma^{2\nu\text{EP}\beta^-}/\Gamma^{2\nu\beta\beta^-}$	$T_{1/2}^{2\nu\beta\beta^-}$ [y]	$T_{1/2}^{2\nu\text{EP}\beta^-}$ [y]
3.809×10^{-18}	1.367×10^{-22}	3.59×10^{-5}	7.10×10^{18}	1.98×10^{23}

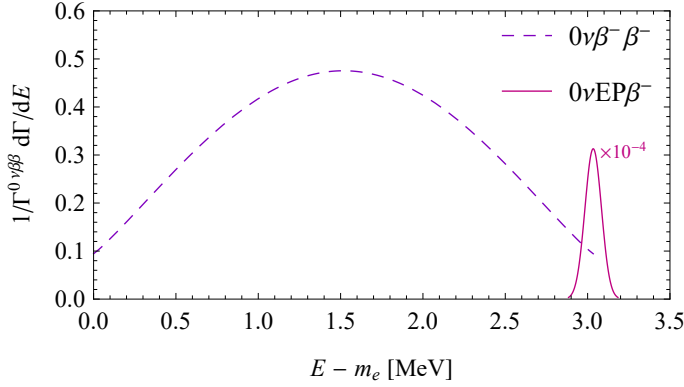


Figure 1. Single-electron $0\nu\beta^-\beta^-$ and $0\nu\text{EP}\beta^-$ spectra $1/\Gamma^{0\nu\beta\beta} d\Gamma/dE$ (the former normalized to unity) as functions of electron kinetic energy $E - m_e$ for the isotope ^{100}Mo ($Q = 3.034$ MeV [17]). The $0\nu\text{EP}\beta^-$ peak is represented by a Gaussian with $\sigma = 50$ keV and scaled by a factor of 10^4 .

Nevertheless, the future double-beta-decay experiments with tracking capability should be able to set limits on the single-electron mode $0\nu\text{EP}\beta^-$ also for other isotopes, most notably SuperNEMO using ^{82}Se as its primary isotope.

In Figure 2, we show the computed single-electron spectra for the $2\nu\beta^-\beta^-$ and $2\nu\text{EP}\beta^-$ modes, defined as the differential decay rates $1/\Gamma d\Gamma/dE$ normalized to unity, for the $0^+ \rightarrow 0^+$ ground-state transition of ^{100}Mo with $Q = 3.034$ MeV [17]. We immediately observe that the single-electron mode $2\nu\text{EP}\beta^-$ exhibits a different shape of the spectrum, which should in turn mani-

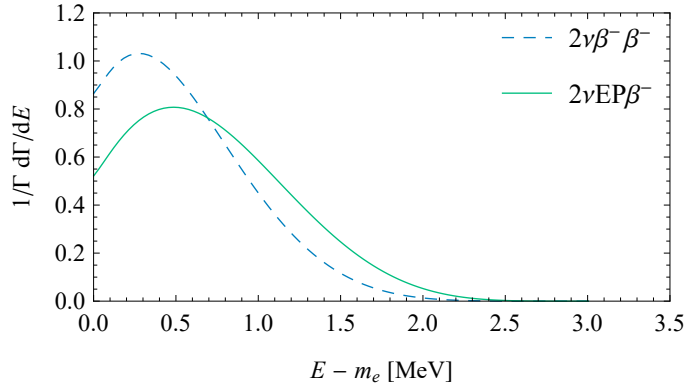


Figure 2. Single-electron $2\nu\beta^-\beta^-$ and $2\nu\text{EP}\beta^-$ spectra $1/\Gamma d\Gamma/dE$ (normalized to unity) as functions of electron kinetic energy $E - m_e$ for the isotope ^{100}Mo ($Q = 3.034$ MeV [17]).

fest through a slight deformation of the measured $2\nu\beta^-\beta^-$ single-electron spectra. With more than 700,000 positive events coming from approximately 7 kg of enriched ^{100}Mo during 3.49 y of exposure (the low-radon phase) and very high signal-to-background ratio [19], we suggest that a thorough reassessment of the NEMO-3 data could provide us with valuable insight into the connection between the atomic physics and mechanisms of the double-beta decay.

4 Conclusion

We have examined new modes of $0\nu\beta^-\beta^-$ and $2\nu\beta^-\beta^-$ in which only one electron is emitted from the atom, the second one being directly produced in the atomic shell of the daughter ion. Such processes would constitute the double-beta-decay counterparts of the bound-state beta decay observed some 25 years ago. We have calculated the phase-space factors, estimated the half-lives and derived the single-electron spectra for the $0^+ \rightarrow 0^+$ ground-state transition of the isotope ^{100}Mo , which was the primary source used in the NEMO-3 experiment. We conclude that while the $0\nu\text{EP}\beta^-$ mode is strongly suppressed, the $2\nu\text{EP}\beta^-$ mode could readily contribute to a slight deformation of the measured NEMO-3 data. The forthcoming experiment SuperNEMO will possess all means to set more stringent limits on both single-electron modes $0\nu\text{EP}\beta^-$ and $2\nu\text{EP}\beta^-$ for other isotopes.

Acknowledgments

This work was supported by the VEGA Grant Agency of the Slovak Republic under Contract No. 1/0922/16, the Slovak Research and Development Agency under Contract No. APVV-14-0524, the Ministry of Education, Youth and Sports of the Czech Republic under the ERDF Grant No. CZ.02.1.01/0.0/0.0/16.013/0001733, the Grant of the Plenipotentiary Representative of the Czech Republic in JINR under Contract No. 203 from 31/03/2017, the RFBR Grant under Contract No. 16-02-01104, and Grant of the Heisenberg–Landau Program under Contract No. HLP-2015-18. The authors express their sincere gratitude towards R. Dvornický for enlightening discussions regarding the atomic-structure calculations.

References

- [1] J.D. Vergados, H. Ejiri, and F. Šimkovic, *Rept. Prog. Phys.* **75** (2012) 106301.
- [2] A. Babič and F. Šimkovic, *AIP Conf. Proc.* **1572** (2013) 7.
- [3] A.S. Barabash, *Nucl. Phys. A* **935** (2015) 52.
- [4] R. Arnold *et al.* (NEMO-3 Collaboration), *Phys. Rev. D* **92** (2015) 072011.
- [5] M. Jung *et al.*, *Phys. Rev. Lett.* **69** (1992) 2164.
- [6] R. Arnold *et al.* (SuperNEMO Collaboration), *Eur. Phys. J. C* **70** (2010) 927.
- [7] S.M. Bilenky and S.T. Petcov, *Rev. Mod. Phys.* **59** (1987) 671.

- [8] C. Patrignani *et al.* (Particle Data Group), *Chin. Phys. C* **40** (2016) 100001, and 2017 update.
- [9] A. Gando *et al.* (KamLAND-Zen Collaboration), *Phys. Rev. Lett.* **117** (2016) 082503.
- [10] J. Kotila and F. Iachello, *Phys. Rev. C* **85** (2012) 034316.
- [11] M.E. Rose, *Relativistic Electron Theory* (Wiley, 1961).
- [12] P. Jönsson, G. Gaigalas, J. Bieroñ, C. Froese Fischer, and I.P. Grant, *Comput. Phys. Commun.* **184** (2013) 2197, GRASP2K version 1.1.
- [13] P. Jönsson *et al.* (The Computational Atomic Structure Group) (2015), a development version of GRASP2K, downloaded from:
<http://ddwap.mah.se/tsjoek/compas/>.
- [14] V.B. Berestetskii, E.M. Lifshitz, and L.P. Pitaevskii, *Quantum Electrodynamics* (Butterworth–Heinemann, 1982).
- [15] M. Doi, T. Kotani, and E. Takasugi, *Prog. Theor. Phys. Suppl.* **83** (1985) 1.
- [16] D. Štefánik, R. Dvornický, F. Šimkovic, and P. Vogel, *Phys. Rev. C* **92** (2015) 055502.
- [17] V.I. Tretyak and Y.G. Zdesenko, *Atom. Data Nucl. Data Tabl.* **80** (2002) 83.
- [18] F. Šimkovic, V. Rodin, A. Faessler, and P. Vogel, *Phys. Rev. C* **87** (2013) 045501.
- [19] A.S. Barabash and F. Piquemal, *Nucl. Phys. News* **23** (2013) 12.